




Article

Production and Characterization of Photocatalytic PEO Coatings Containing TiO₂ Powders Recovered from Wastes

Luca Pezzato ^{1,2,*}, Elena Colusso ¹, Pietrogiovanni Cerchier ^{1,2}, Alessio Giorgio Settimi ^{1,2} and Katya Brunelli ¹

¹ Department of Industrial Engineering, University of Padova, Via Marzolo 9, 35131 Padova, Italy

² 9-Tech srl, Via Triestina Bassa 74, 30020 Eraclea, Italy

* Correspondence: luca.pezzato@unipd.it; Tel.: +39-0498275503

Abstract: In this work, the possibility of incorporating TiO₂ titanium dioxide particles derived from the recycling process of photovoltaic panels into PEO coatings was investigated. These particles constitute the main filler of the polymer constituting the rear part of the panels, and are characterized by possessing photocatalytic properties. The particles were added in different quantities to the electrolyte (a basic solution containing sodium silicate). The incorporation into the PEO coating produced on an aluminum alloy 1050, and the possibility of conferring photocatalytic properties to the surface of the samples were studied. The different samples were first characterized by optical microscope analysis, SEM and XRD and from the point of view of corrosion resistance by means of potentiodynamic tests. The photocatalytic properties of the samples were evaluated by monitoring the degradation of aqueous solutions of methylene blue exposed to a UV lamp. The particles have been successfully incorporated into the coating, and their presence does not alter the corrosion properties, which are improved compared to the uncoated sample. The particles, initially composed of a mixture of rutile and anatase, are instead transformed into rutile after incorporation due to the locally very high temperatures that can occur during the PEO process. In the samples obtained with higher quantities of titanium dioxide particles (60 and 80 g/L), a significant photocatalytic effect is observed with a significant reduction of methylene blue.

Keywords: plasma electrolytic oxidation; aluminum alloys; titanium oxide; photocatalytic; corrosion; circular economy



Citation: Pezzato, L.; Colusso, E.; Cerchier, P.; Settimi, A.G.; Brunelli, K. Production and Characterization of Photocatalytic PEO Coatings Containing TiO₂ Powders Recovered from Wastes. *Coatings* **2023**, *13*, 411. <https://doi.org/10.3390/coatings13020411>

Academic Editor: Alexandru Enesca

Received: 18 January 2023

Revised: 7 February 2023

Accepted: 9 February 2023

Published: 11 February 2023



Copyright: © 2023 by the authors. Licensee MDPI, Basel, Switzerland. This article is an open access article distributed under the terms and conditions of the Creative Commons Attribution (CC BY) license (<https://creativecommons.org/licenses/by/4.0/>).

1. Introduction

The Plasma Electrolytic Oxidation (PEO) process is a surface treatment conceptually similar to the conventional anodizing process, but in which different electrolytes are used (neutral-basic alkaline instead of acid) and higher voltages and currents are employed [1,2].

Key to the process are the anodic micro-discharges formed over the metal surface, due to the fact that the potential is higher than the dielectric breakdown. These discharges produce the formation of the discharge channels (that after will partially result in pores in the final coating) and permit growth on an oxide ceramic film constituted not only by the oxide of the substrate but also by compounds coming from the electrolyte that remain trapped in the discharge channels [3]. This, together with the extremely rapid melting and re-solidification process that produces the formation of amorphous and nanocrystalline phases, permits the obtaining of coatings with improved corrosion and tribological properties in comparison with the ones obtained through traditional anodizing [4].

Some of the main characteristics of the coatings obtained with PEO are the high porosity of the outermost layer and the possibility of incorporating particles or compounds dispersed within the electrolyte directly into the coating, thus functionalizing the metal surface accordingly [5].

Considering the incorporation of particles suspended into the electrolyte, O'Hara et al. [6] recently demonstrated that the main mechanism of incorporation is the sweeping of suspended particulate into active discharge sites immediately after plasma collapse. Hence, the particles are trapped in the discharge channels; the incorporation could occur due to inert or reactive incorporation, depending by the chemical nature of the particles. Particles with a high melting point are incorporated inertly into the PEO layer. Particles with a low melting point are instead reactively incorporated into the coating due to a rapid melting/solidification process, forming generally amorphous phases that can significantly modify the corrosion performance of the coating [7].

Clearly the type of compound/particles incorporated determines the particular functional property of the surface: inhibitors to improve the corrosion properties [8]; compounds to increase the biocompatibility of the surfaces [9], hard particles to improve the wear properties [10]; and photocatalytic compounds to confer this property to the surface.

The study of the photocatalysis and the production of photocatalytic surfaces has attracted increasing interest in recent years, due to the key role that photocatalytic compounds can play in the reduction of pollution and of energy consumption, which are among the problems of the 21st century [11–15].

In particular, an often-employed compound that is characterized by photocatalytic properties is titanium dioxide, in particular in the form of anatase [16–18]. In fact, TiO₂ properties depend strongly on the particle size, crystal structure, morphology and crystallinity, and TiO₂-based coatings can be employed for a wide range of applications, from protection or corrosion to optical properties passing through the photocatalytic activity, depending by the crystalline form employed [19–22].

The possibility of conferring photocatalytic properties on PEO coatings was already quite widely studied in the literature and in particular a lot of works are based on the photocatalytic properties of titanium dioxide. Stojadinovic et al. [23] prepared TiO₂:Eu³⁺ coatings by plasma electrolytic oxidation (PEO) in an electrolyte containing Eu₂O₃ powder using titanium as substrate, obtaining good photocatalytic activity. Lin et al. [24] produced highly photocatalytic TiO₂-containing coatings over flexible Ti foils using phosphate-based electrolyte. Lu et al. [25] achieved photocatalytic activity of PEO coatings produced on magnesium alloy substrate via the introduction of anatase (TiO₂ particles) to the treatment bath. They found that the photocatalytic performance of the coating is primarily related to the anatase content on the coating surface, and can be modified by varying the process parameters. Considering aluminum alloy substrate, Tadic et al. [26] reported the rapid deposition of TiO₂ nanoparticles on aluminum by plasma electrolytic oxidation in a Na₂SiO₃·5H₂O water-based electrolyte with the addition of TiO₂ nanoparticles and Na₂WO₄·2H₂O, obtaining notable photocatalytic activity for the photodecomposition of MO (Metil-Orange).

In all the works carried out in the literature, in order to confer photocatalytic properties to the coatings, expensive compounds were added into the electrolyte. In this work, and, to the best of our knowledge, for the first time, titanium dioxide powders were recovered from waste and after employed to functionalize PEO coatings produced on aluminum alloys. In detail, the aim of this study was to analyze the possibility of incorporating titanium dioxide particles, obtained from the recovery process of end-of-life solar panels into PEO coatings produced on 1050AA.

The particles, in an idea of circular economy, were recovered from End-of-Life (EoL) Photovoltaic (PV) panels and incorporated into PEO coatings with the aim of conferring photocatalytic properties to the coated surface. In fact, in order to block ultraviolet (UV) from the back side and redirect reflected sunlight (albedo) from the front side of a PV module, white pigments such as titanium dioxide (TiO₂) and barium sulfate (BaSO₄) are widely used in back sheet layers to modify the optical properties of polymeric layers [27,28].

The particles, in detail, were recovered from the back sheets of the EoL PV panels through a process performed in a pilot plant dedicated to PV recycling, which is described by Cerchier et al. [29]. As we will discuss in the manuscript, the particles are initially

composed of a mixture of rutile and anatase, and they turn into a unique rutile phase after PEO incorporation.

The photocatalytic properties of the recovered particles were, therefore, first verified themselves and subsequently those of the particles-containing coatings were analyzed. Despite the crystalline transformation, it was observed that the photocatalytic properties of the coatings are strongly dependent on the quantity of incorporated particles. For high contents of incorporated particles, the coated surface possesses acceptable photocatalytic properties even if the temperatures reached during the PEO process led to the transformation of anatase into rutile and, therefore, to the loss of part of the photocatalytic capacity.

2. Materials and Methods

2.1. Coatings Preparation

The 1050 aluminum alloy samples (nominal composition reported in Table 1) were used as substrate for PEO coatings.

Table 1. Chemical composition of 1050AA (wt%).

Al%	Si%	Fe%
99.5	0.25	0.25

The samples, before the PEO treatment, were polished with standard metallographic technique using a grinding step with abrasive papers (500, 800, 1200 and 4000 grit) and a polishing step with cloths and diamond suspensions (6 μm and 1 μm). The samples were then degreased using acetone in ultrasound. Polishing was performed to obtain uniform superficial conditions between the samples before PEO treatment. PEO coatings were produced using a TDK-Lambda DC power supply of 400 V/8 A capacity working in galvanostatic mode at the fixed current density of 0.5 A/cm². The treatments were performed in pulsed current mode, with a frequency of 20 Hz and a duty cycle of 50%, obtained with a proper relay. All the samples were treated for 4 min.

During the treatments, the substrate working as anode and the cathode was a carbon steel mesh. An aqueous alkaline solution containing 25 g/L of Na₂SiO₃ and 2.5 g/L of NaOH was employed as an electrolyte to produce the standard PEO samples.

The effect of different quantities (5, 10, 20, 40, 60 or 80 g/L) of recovered titanium dioxide particles on the microstructure, corrosion and photocatalytic properties of the coatings was studied. Additionally, a sample without particles (0 g/L) was produced and characterized as a comparison for all the properties. The titanium dioxide particles were maintained in suspension through magnetic stirring.

The photocatalytic activity of the powders was preliminary tested (see Figure S1, Supporting Information) to prove potential application in dye degradation.

The particles were recovered from the back sheets of a uniform batch of EoL PV panels, in order to be sure that only TiO₂ was contained in the back sheet (thereby avoiding excessive contamination of BaSO₄ powder).

According to the recycling process described by Cerchier et al. [29], the PV panels were subjected to incineration at high temperature (>450 °C) that was performed in a dedicated furnace designed and constructed by the University of Padova in the framework of the ReSiELP research project. The performed process eliminated the EVA encapsulant, which keeps together the different layers of which the panels are made, thus allowing the separation of the materials contained in the PV modules. During this process, the polymeric back sheets of the PV panels were also incinerated, releasing the TiO₂ powder contained inside them.

After heating treatment and cooling of the treated material, this powder was sucked up using an ash vacuum cleaner. The powder was then sieved with 1 mm mesh to remove any residues of glass or photovoltaic cells accidentally aspirated. The resulting particles, as can be observed from SEM observation in Figure 1, were characterized by

sub-micrometric dimensions and spherical shape. XRD analysis performed on the particles (Figure 2) evidence the presence of titanium dioxide, both in the forms of rutile and anatase, but also other compounds such as barium sulphate, silicon and silicon oxide are present, as can be predicted due to the fact that the particles are recovered from PV wastes.

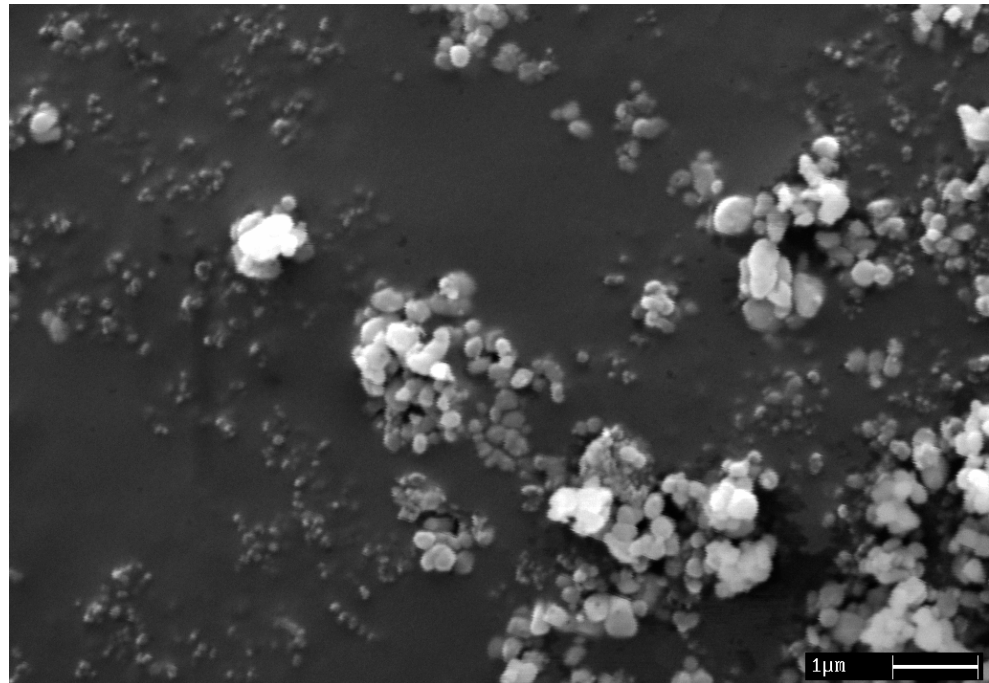


Figure 1. SEM images of the particles recovered from PV panels employed to functionalize PEO coatings.

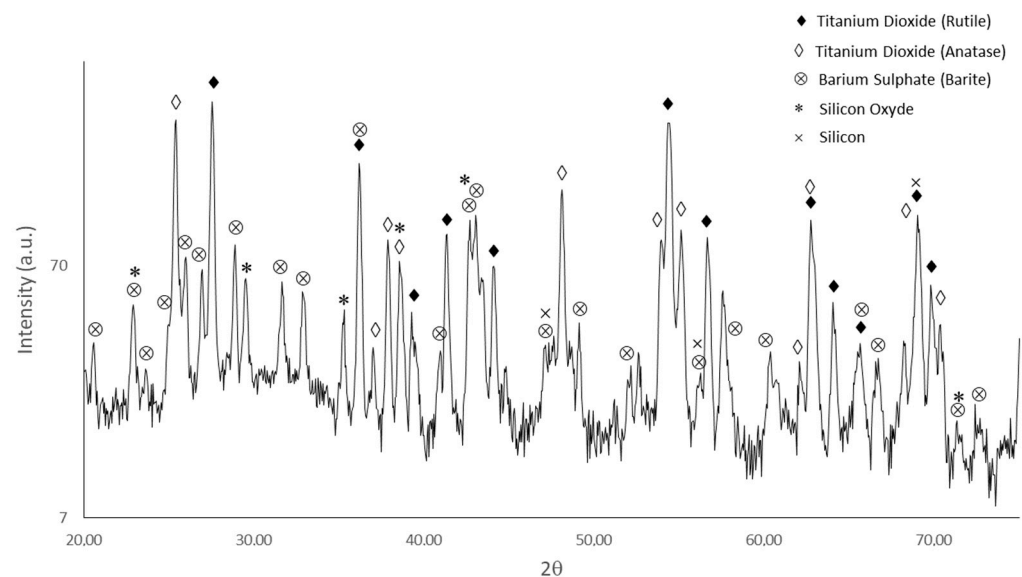


Figure 2. XRD spectra of the particles recovered from PV panels employed to functionalize PEO coatings.

The electrolyte with the particles dispersed was also maintained at ambient temperature by a thermostatic bath and magnetic stirred. After the treatment, the samples were washed with deionized water and dried with compressed air.

2.2. Coatings Characterization

PEO treated samples were cut along the cross section, mounted in epoxy resin and polished. A Cambridge Stereoscan 440 scanning electron microscope (Leica Microsystem S.r.l., Milan, Italy) equipped with a Philips PV9800 EDS (Leica Microsystem S.r.l., Milan, Italy), was used to analyze both the surface and the cross section of the samples in order to evaluate composition, thickness, adhesion and microstructure of the coatings.

Phase composition of the coatings was performed with a Siemens D500 X-ray diffractometer (Siemens, Munich, Germany) with a nickel-filtered Cu-K α radiation source ($\lambda = 0.15405$ nm), operating at 40 kV and 30 mA. Identification of the phases was performed with the PDF-2 database.

Photocatalytic tests were performed in a glass beaker using methylene blue (MB, 15 mg/L in water, 50 mL) as a model compound [30,31]. Before experiments, the initial absorbance of the solution was measured using a UV-vis spectrophotometer Jasco V570, (JASCO EUROPE S.R.L., Lecco, Italy) between 350 and 850 nm. We verified the adsorption activity of the samples by leaving them in the dark for 30 min before irradiation. The samples were then perpendicularly irradiated for 60 min with a UV lamp LC5 Hamamatsu, 10 mW/cm², (Hamamatsu Corporation, Bridgewater, New Jersey, USA). After a given amount of time, a 3 mL MB test portion was taken out of the beaker and the change in absorbance was measured at 664 nm. After each measurement, the probe solution was returned to the photocatalytic reactor. Before photocatalysis measurements, the MB solution was tested for photolysis in the absence of the photocatalyst to examine its stability. The degradation efficiency χ was obtained from the following Equation (1):

$$\chi = \frac{C_0 - C_t}{C_0} * 100 \quad (1)$$

where C_0 is the initial concentration of MB, and C_t is the concentration at a given time t [26]. The degradation rate constant k was also calculated from Equation (2):

$$\ln (C_0/C_t) = kt \quad (2)$$

where k is the apparent first-order rate constant and t is the illumination time [32].

Additionally, corrosion performances of the samples and the effect of the presence of the titanium dioxide particles were briefly performed by means of potentiodynamic polarization (PDP) tests. These preliminary tests were performed with comparative purposes in order to understand whether the presence of the particles can modify the corrosion behavior in comparison with the sample PEO treated without particles and with the untreated sample. An AMEL 2549 Potentiostat (Amel Electrochemistry S.r.l., Milan, Italy), was employed for PDP tests that were performed in a solution 0.1 M Na₂SO₄ and 0.05 M NaCl, to simulate a moderate aggressive environment containing both sulphates and chlorides. A saturated calomel electrode was used as a reference electrode (SCE) and a platinum electrode as a counter electrode. The tests were performed after 30 min of OCP stabilization with a scan rate of 0.5 mV s⁻¹ in a potential range from -1.5 to -0.8 V. Every measure was repeated three times in order to assure the reproducibility of the test. Additionally, an untreated sample and a sample PEO treated without particles were tested as a comparison.

Finally, we measured the static water contact angle (WCA) of the samples by the sessile-drop method using a home-made set-up consisting of a DCC1545M CMOS sensor camera (Thorlabs GmbH[®], Bergkirchen, Germany) and MVL7000 sensor lens (Thorlabs GmbH[®], Bergkirchen, Germany) and a dispensing microfluidic syringe. An average of 3 points was measured.

3. Results

3.1. Microstructural Characterization

A first visual inspection of the samples, reported in Figure 3, evidenced that the recovered titanium dioxide particles produce the formation of black zones on the surface

of the sample, in comparison with the one produced without the addition of particles (Figure 3a). The number of black zones increased with the increase of particle content. Additionally, the uniformity in the distribution of the particles increased with the number of particles. In fact, in the samples 5, 10 and 20 g/L a strong disuniformity in particle distribution can be noted, whereas in the samples 40, 60 and 80 g/L almost the whole surface is covered with particles (except for the zone in the right-bottom, probably due to the flow of the particles due to magnetic stirring).

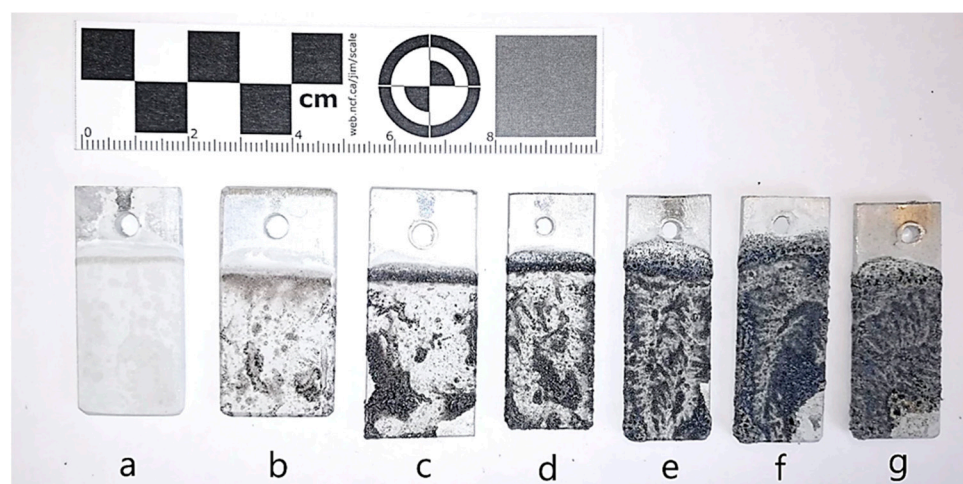


Figure 3. Visual observation of the various PEO treated samples: 0 g/L (a), 5 g/L (b), 10 g/L (c), 20 g/L (d), 40 g/L (e), 60 g/L (f) and 80 g/L (g).

The samples show a hydrophilic behavior, with an average water contact angle of 26° for the 0 g/L. The addition of the nanoparticles decreases the WCA up to 15° – 10° for the 40, 60 and 80 g/L compositions, while a higher variability of the values was observed for the lower particle content, consistent with the high disuniformity. The results are summarized in Table S1 in the Supporting Information.

All the samples were also observed both on the surface and along the cross section by SEM, and the results are reported in Figures 4 and 5, respectively.

Considering the surfaces of the samples (Figure 4), the typical microstructure of PEO coatings with the presence of the pores and of the pancake structures can be noted, due to the discharge phenomena that occur during the process. This resulted in accordance with the current literature regarding PEO coatings [33,34], due to the fact that the discharge channels resulted in pores on the surface of the samples. Comparing the surfaces of the different samples, no significant differences in the surface morphology can be observed between the samples obtained without titanium dioxide powders (Figure 4a) and the ones obtained with TiO_2 addition. In detail, the pores that resulted from the PEO treatment were not filled by the powders, which did not result in them being inertly incorporated into the coating. However, the presence of titanium compounds on the surfaces of the samples resulted in confirmation by EDS analysis, as reported in Table 2. In detail, the quantity of Ti increased with the increase of TiO_2 powders in the electrolyte (11.1% in the sample 80 g/L vs. 4.3% in the sample 5 g/L), indicating that more titanium oxide enters into the coating, increasing its quantity into the electrolyte.

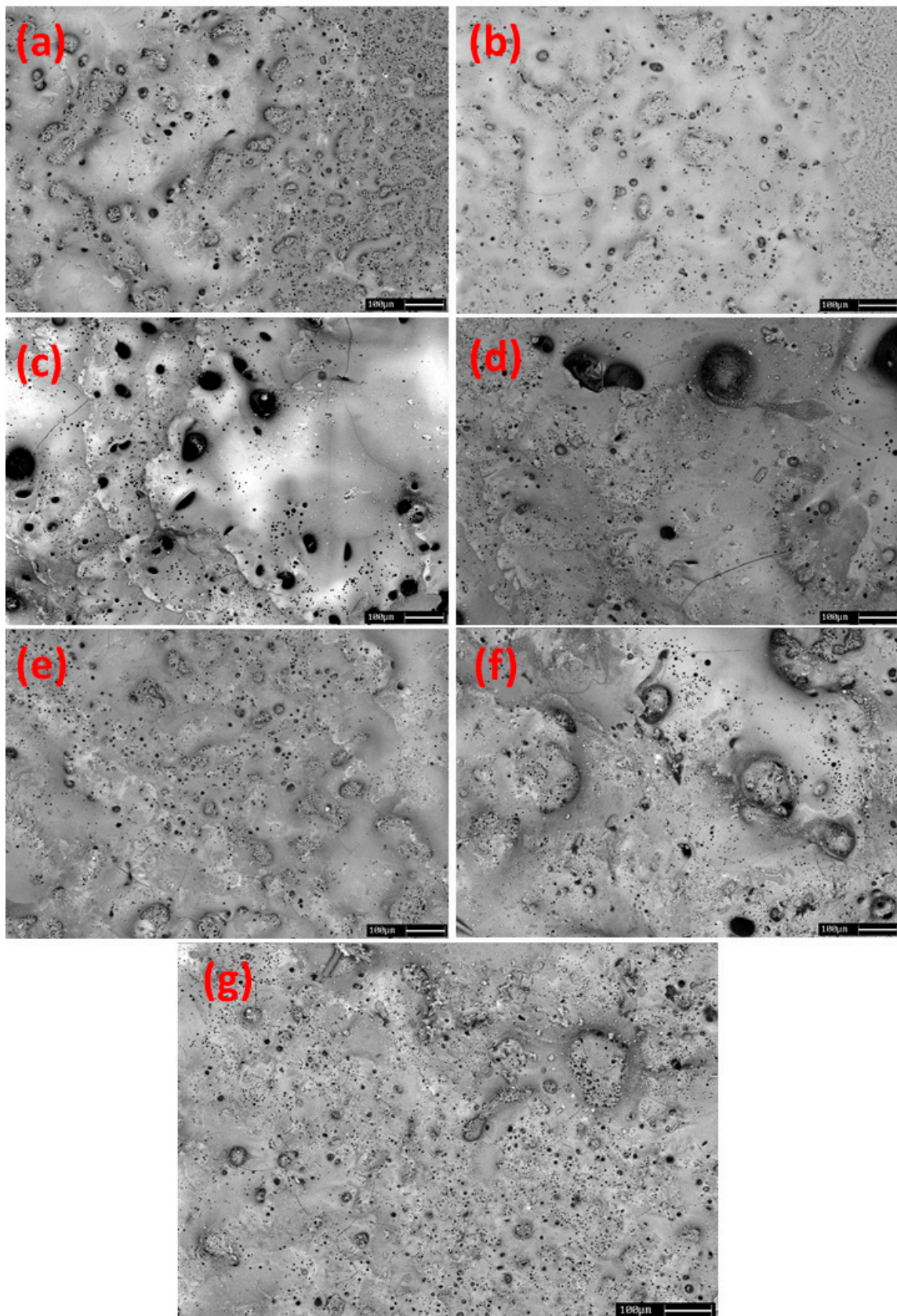


Figure 4. SEM micrographs of the surfaces of the various PEO treated samples: 0 g/L (a), 5 g/L (b), 10 g/L (c), 20 g/L (d), 40 g/L (e), 60 g/L (f) and 80 g/L (g).

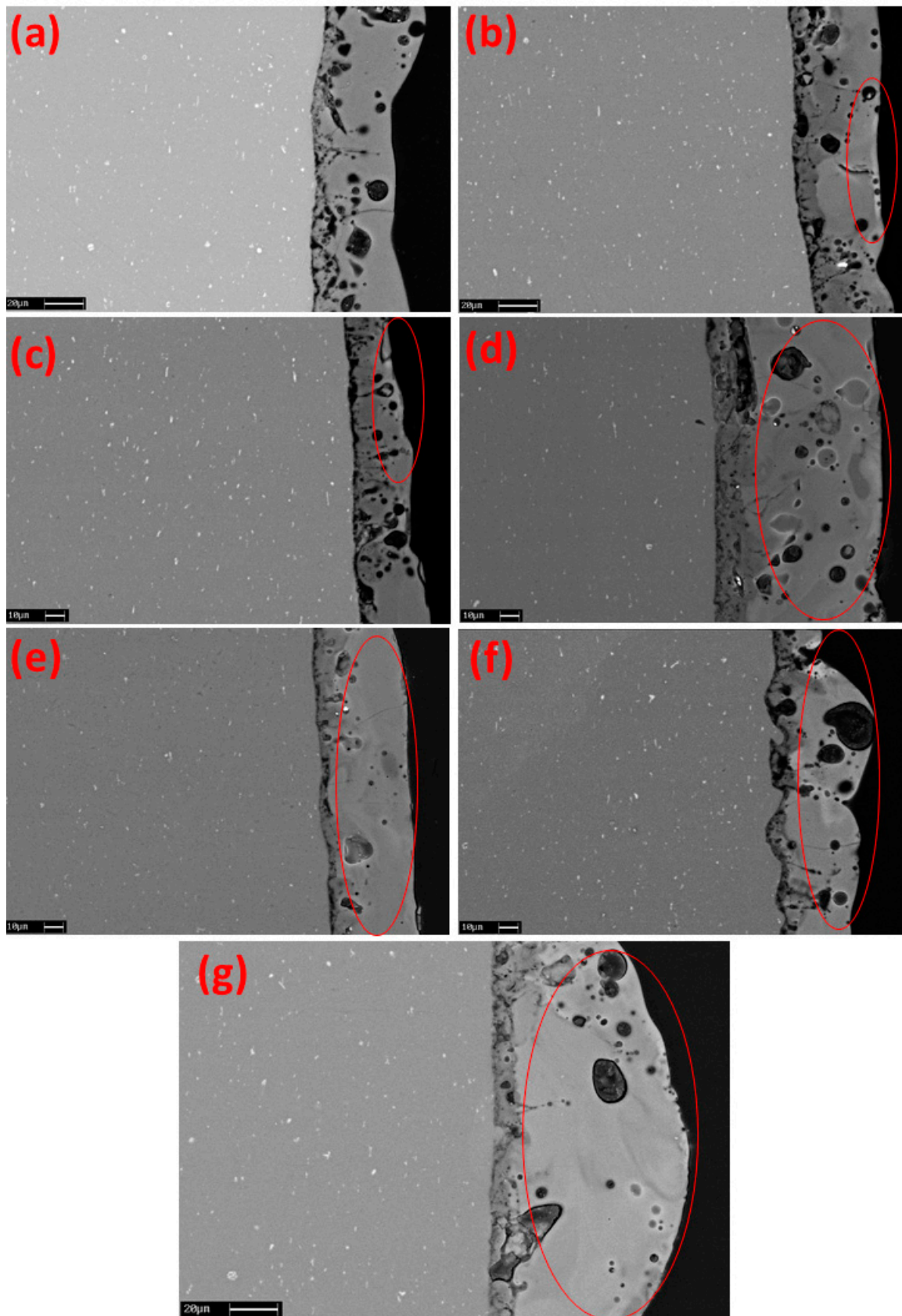


Figure 5. SEM micrographs of the cross sections of the various PEO treated samples: 0 g/L (a), 5 g/L (b), 10 g/L (c), 20 g/L (d), 40 g/L (e), 60 g/L (f) and 80 g/L (g).

Table 2. Results of semi-quantitative EDS analysis (wt%) performed on the surface of the different samples.

Element	0 g/L	5 g/L	10 g/L	20 g/L	40 g/L	60 g/L	80 g/L
O%	49.2	49.1	49.3	48.3	49.5	50.8	49.6
Na%	1.6	3.1	3.9	5.2	4.9	6.2	6.9
Al%	19.1	13.4	11.3	8.1	8.9	7.0	6.1
Si%	29.8	26.9	23.6	22.5	22.5	7.0	20.4
Ca%	0.2	3.2	5.8	7.3	4.3	7.0	5.9
Ti%	0.1	4.3	6.1	8.6	9.9	7.0	11.1

In order to deeply analyze the microstructure of the coatings and to verify the effect of the addition of titanium oxide powders, the cross sections of the samples were also analyzed at the SEM and the results are reported in Figure 5. Additionally, in this case EDS analysis was performed and the semi-quantitative results can be found reported in Table 3. First of all, it can be observed that the presence of the particles does not modify the morphology of the coating, which remains porous and with good adhesion to the substrate (see Figure 5a of the sample, obtained without particles with the others). The way in which the particles are effectively incorporated within the coating through a partially reactive mechanism, which leads them to re-solidify within the coating itself, can also be observed. In fact, from the images obtained with backscattered electrons, it can be observed that the areas rich in TiO₂, lighter than the others and highlighted by red circles in the images, increase as the particle content increases. In particular, the presence of these zones resulted particularly evidently in the samples obtained with 60 g/L (Figure 5f) and 80 g/L (Figure 5g) of particles. The partially reactive mechanism of incorporation of the titanium dioxide powders can be related to the melting point of TiO₂, which is around 1800 °C [35]. According to Lee et al. [36], the temperature of arc plasma ranges, in fact, between 1800 and 2370 °C, and this will produce at least partial melting of the titanium dioxide during the process, causing the reactive incorporation into the coating.

Table 3. Results of semi-quantitative EDS analysis (wt%) performed on the cross-sections of the different samples.

Element	0 g/L	5 g/L	10 g/L	20 g/L	40 g/L	60 g/L	80 g/L
O%	39.7	48.5	39.7	41.4	37.6	37.9	36.3
Na%	1.1	1.9	0.0	2.5	2.0	3.2	1.2
Al%	13.2	12.3	14.7	15.3	15.4	12.7	12.3
Si%	46.0	33.8	26.0	31.2	29.3	28.8	28.1
Ca%	0.0	1.8	5.0	3.2	3.1	7.3	5.8
Ti%	0.0	1.7	14.6	6.4	12.6	10.1	16.3

The successful incorporation of the particles during the PEO treatment is also demonstrated by the XRD analyses reported in Figure 6 (sample 0 g/L of particles) and Figure 7 (sample 80 g/L of particles). Comparing the two spectra, it can, in fact, be noted that in the sample obtained with 80 g/L of particles the rutile peaks are clearly observable, as well as those of alumina (from the PEO coating) and aluminum (from the substrate). In the sample obtained without particles the rutile peaks are not visible. By comparing the spectrum of Figure 7 with the one related to the particles shown in Figure 2, it can be observed that, following the incorporation, the crystalline form of anatase, which was instead present in the particles, is no longer visible in the coating. In fact, only rutile is visible in the PEO coating. This is due to the fact that the high temperatures reached during the PEO treatment (even if only locally and for the short duration of the discharges) cause the transformation of anatase into rutile. In fact, this transformation generally takes place at temperatures around 900 °C–1000 °C [37], decidedly lower than those locally reachable during the process of formation of the PEO discharges (about 1800 °C–2370 °C [36]). This

transformation is not favorable for obtaining surfaces with photocatalytic characteristics, since the photocatalytic effect of anatase is greater than that of rutile. The fact that the PEO treatment produces the transformation of anatase in rutile is, however, of high scientific interest, because it is indirect proof of the temperatures reached during the PEO treatment.

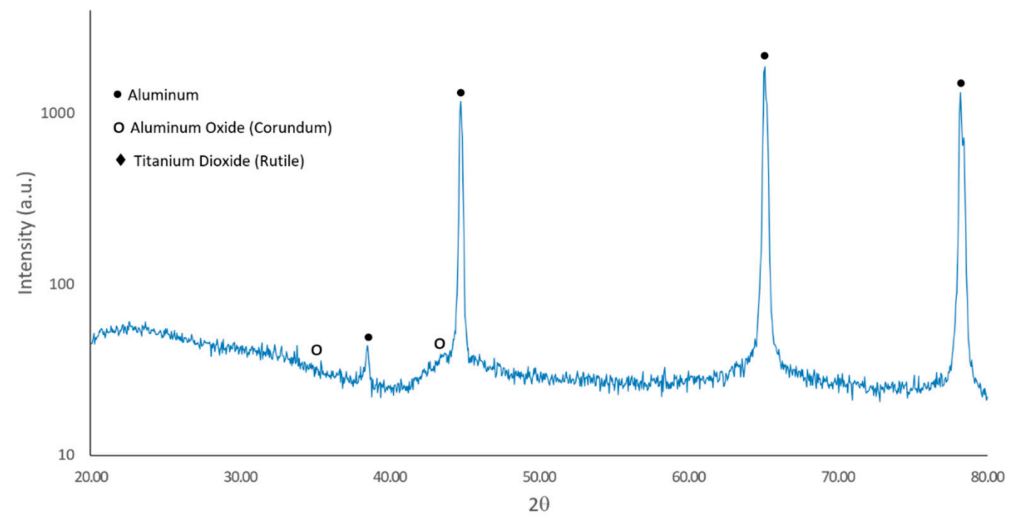


Figure 6. XRD spectra of the sample PEO treated with 0 g/L of particles.

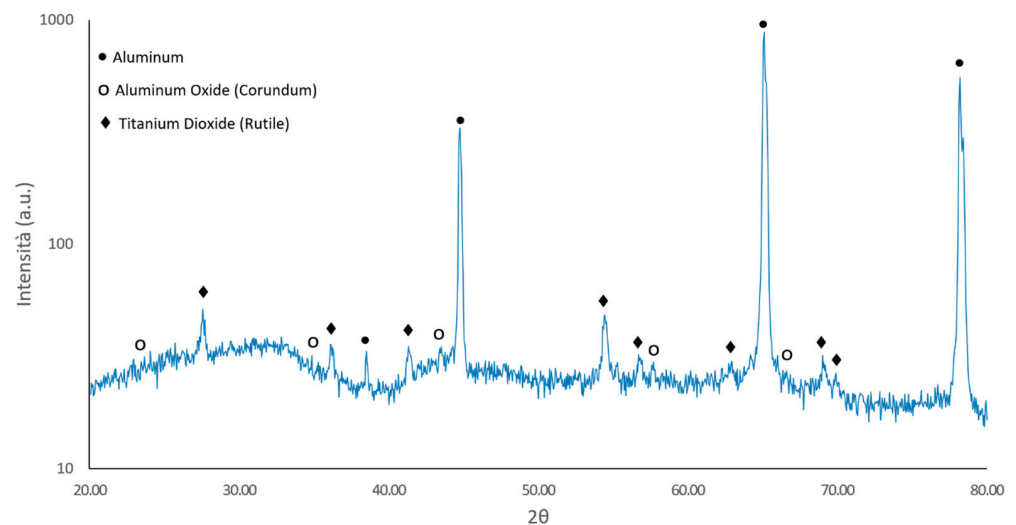


Figure 7. XRD spectra of the sample PEO treated with 80 g/L of particles.

3.2. Corrosion Resistance Evaluation

The corrosion resistance of the coated samples was also evaluated through potentiodynamic polarization tests and the results are presented in Figure 8. First of all, it can be observed that all the coated samples are characterized by a higher resistance to corrosion than the uncoated sample since, following the treatment, a marked drop in the corrosion current and therefore in the corrosion rate is observed. On the other hand, a definite trend that links the quantity of particles with the corrosion properties is not observed. In fact, all the samples treated with the presence of titanium dioxide particles show a behavior similar to each other and similar to that of the PEO treated sample without particles, in terms of corrosion current density. This can be connected to the fact that, as observed from the SEM images, the presence of the particles does not lead to large microstructural or morphological variations in the coating, thus not involving substantial variations in the corrosion behavior. Moreover, as previously observed, the titanium dioxide particles do not fill the pores that characterize the PEO layer, thus not improving the corrosion resistance.

The effect of the particles' addition on the corrosion properties is, in fact, strongly related to the microstructural changes that they produce in terms of densification of the coatings. When the presence of the particles does not lead to coating densification, the corrosion properties can remain un-modified or can even be reduced [38].

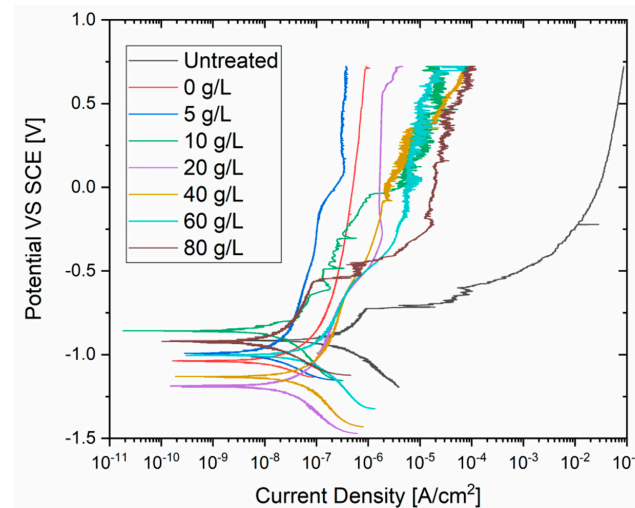


Figure 8. Results of the potentiodynamic polarization tests performed on the different PEO treated samples and comparison with the untreated one.

3.3. Photocatalytic Properties

The photocatalytic properties of the samples were evaluated by monitoring the change in absorbance of the MB solution with the time of irradiation at the 664 nm wavelength (Figure 9a). Before the irradiation, we verified the adsorption of dye from the samples in the dark (see Figure S2 in the Supporting Information). As expected, a slight reduction of the dye concentration was observed, due to the presence of porosity in the PEO coatings (Figure S2, Supporting Information). However, the effect is much lower if compared to the degradation under UV light. As visible from the results in Figure 9b, the degradation of the MB is accelerated in the presence of PEO samples with TiO₂ NPs.

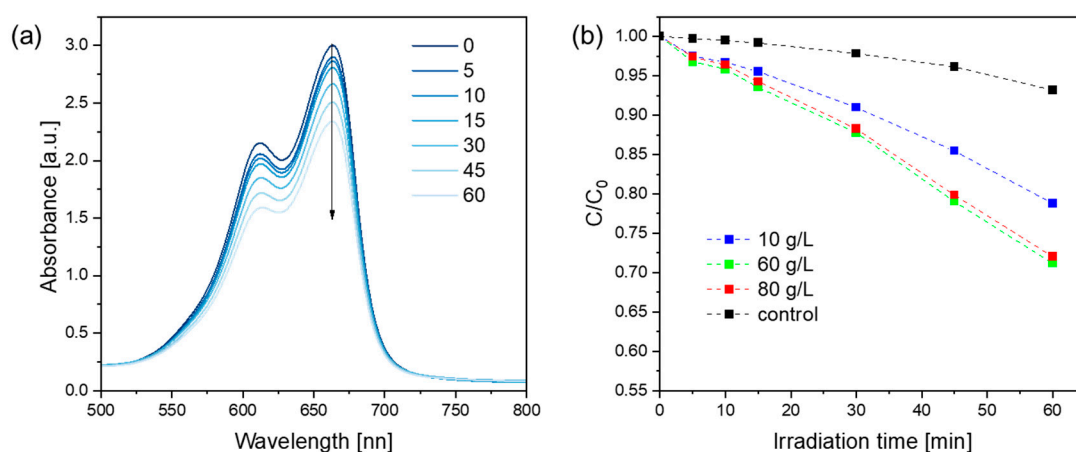


Figure 9. (a) Variation of MB absorbance spectra with irradiation time in presence of PEO 60 g/L; (b) photocatalytic degradation of MB as a function of irradiation time for different PEO samples and for the control experiment (UV light, no sample).

The calculated rate constants were 0.0038, 0.0055 and 0.0054 min⁻¹ for PEO samples prepared with 10, 60 and 80 g/L, respectively (see Table 4). These rates are about three to five times higher compared to the control condition without samples. After 60 min of

irradiation, the percentage of degradation was estimated to be about 30% for PEO 60 and 80 g/L, 10% more compared with the sample prepared with a lower amount of TiO₂. The results are comparable with the values reported in the literature for other PEO coatings with titania nanoparticles [39]. The increased efficiency for 60 and 80 g/L agrees with the cross-section SEM images, which showed higher incorporation of TiO₂ particles in these conditions. The improvement in the photocatalytic efficiency could be also related to the formation of oxygen vacancies on the surface during the PEO process [40].

Table 4. Rate constant k and percentage of degradation χ after 60 min of MB in the presence of PEO samples and without it.

Sample	k [min ⁻¹]	χ [%]
Control	0.0011	6.78
10 g/L	0.0038	21.20
60 g/L	0.0055	28.81
80 g/L	0.0054	27.97

It can therefore be stated that, despite the transformation of anatase into rutile, the samples containing high quantities of titanium dioxide (60 and 80 g/L) show significant photocatalytic activity. Considering that the particles are waste from the recycling process of end-of-use photovoltaic panels, the result is promising for a possible future use of the particles themselves.

4. Conclusions

In conclusion, the obtained results can be summarized as follows:

- Titanium dioxide particles were successfully incorporated into PEO coatings on 1050 aluminum alloy. The incorporation takes place by simply adding the particles to the electrolyte used during the process by exploiting the formation of discharge channels during the PEO process. The incorporation is partially reactive, as the particles lose their original shape and re-solidify in the coating, due to the fact that the temperatures reached during the treatment are above the melting point of titanium dioxide;
- The presence of particles does not lead to large microstructural variations in the coating, which in any case remains rich of pores that are not sealed by the presence of the particles;
- The incorporation instead leads to significant changes in the crystalline structure of the particles. The particles, initially made up of a mixture of rutile and anatase, are only made up of rutile after incorporation due to the very high local temperatures obtained during the PEO process;
- All coated samples are characterized by superior corrosion resistance if compared to the uncoated sample. The quantity and the presence of the particles does not influence the corrosion resistance of the coated samples. In fact, the behavior of the samples obtained with the particles is comparable to that of the sample without particles.
- Despite the unfavorable anatase–rutile transformation that occurs during the incorporation, the presence of the particles confers photolytic properties on the surface of the coated samples. These characteristics increase as the particle content increases, and are highest in samples obtained with 60 and 80 g/L of particles in the electrolyte. For these samples, a capacity to reduce methylene blue after 60 min of around 30% is observed;
- The use of titanium dioxide particles recovered from the recycling of end-of-use photovoltaic panels as an additive for the production of PEO coatings with photocatalytic properties is, therefore, a promising application in an idea of circular economy.

Supplementary Materials: The following supporting information can be downloaded at: <https://www.mdpi.com/article/10.3390/coatings13020411/s1>, Figure S1: Photocatalytic activity of TiO₂ powder from wastes under UV illumination; Figure S2: Adsorption of methylene blue in the dark by PEO samples; Table S1: Water contact angles of the different PEO samples.

Author Contributions: Conceptualization, L.P. and P.C.; methodology, L.P. and K.B.; software, A.G.S.; validation, A.G.S.; formal analysis, A.G.S.; investigation, L.P., A.G.S., E.C. and P.C.; resources, L.P. and K.B.; data curation, L.P. and E.C.; writing—original draft preparation, L.P. and E.C.; writing—review and editing, K.B.; visualization, A.G.S.; supervision, K.B.; project administration, K.B. and L.P.; funding acquisition, K.B. All authors have read and agreed to the published version of the manuscript.

Funding: Project supported by the BIRD 2020 program of the University of Padova (Project BIRD202558/20).

Institutional Review Board Statement: Not Applicable.

Informed Consent Statement: Not Applicable.

Data Availability Statement: The raw/processed data required to reproduce these findings cannot be shared at this time as the data also form part of an ongoing study.

Conflicts of Interest: The authors declare no conflict of interest.

References

1. Yerokhin, A.L.; Lyubimov, V.V.; Ashitkov, R.V. Phase formation in ceramic coatings during plasma electrolytic oxidation of aluminium alloys. *Ceram. Int.* **1998**, *24*, 1–6. [[CrossRef](#)]
2. Matykina, E.; Arrabal, R.; Mohedano, M.; Mingo, B.; Gonzalez, J.; Pardo, A.; Merino, M.C. Recent advances in energy efficient PEO processing of aluminium alloys. *Trans. Nonferrous Met. Soc. China* **2017**, *27*, 1439–1454. [[CrossRef](#)]
3. Clyne, T.W.; Troughton, S.C. A review of recent work on discharge characteristics during plasma electrolytic oxidation of various metals. *Int. Mater. Rev.* **2019**, *64*, 127–162. [[CrossRef](#)]
4. Pezzato, L.; Vranescu, D.; Sinico, M.; Gennari, C.; Settimi, A.G.; Pranovi, P.; Brunelli, K.; Dabalà, M. Tribocorrosion properties of PEO Coatings produced on AZ91 magnesium alloy with silicate- or phosphate-based electrolytes. *Coatings* **2018**, *8*, 202. [[CrossRef](#)]
5. Lu, X.; Mohedano, M.; Blawert, C.; Matykina, E.; Arrabal, R.; Kainer, K.U.; Zheludkevich, M.L. Plasma electrolytic oxidation coatings with particle additions—A review. *Surf. Coat. Technol.* **2016**, *307*, 1165–1182. [[CrossRef](#)]
6. O'Hara, M.; Troughton, S.C.; Francis, R.; Clyne, T.W. The incorporation of particles suspended in the electrolyte into plasma electrolytic oxidation coatings on Ti and Al substrates. *Surf. Coat. Technol.* **2020**, *385*, 125354. [[CrossRef](#)]
7. Lu, X.; Sah, S.P.; Scharnagl, N.; Störmer, M.; Starykevich, M.; Mohedano, M.; Blawert, C.; Zheludkevich, M.L.; Kainer, K.U. Degradation behavior of PEO coating on AM50 magnesium alloy produced from electrolytes with clay particle addition. *Surf. Coat. Technol.* **2015**, *269*, 155–169. [[CrossRef](#)]
8. del Olmo, R.; Mohedano, M.; Visser, P.; Matykina, E.; Arrabal, R. Flash-PEO coatings loaded with corrosion inhibitors on AA2024. *Surf. Coat. Technol.* **2020**, *402*, 126317. [[CrossRef](#)]
9. Pezzato, L.; Brunelli, K.; Diodati, S.; Pigato, M.; Bonesso, M.; Dabalà, M. Microstructural and corrosion properties of hydroxyapatite containing peo coating produced on az31 mg alloy. *Materials* **2021**, *14*, 1531. [[CrossRef](#)]
10. Pezzato, L.; Lorenzetti, L.; Tonelli, L.; Bragaglia, G.; Dabalà, M.; Martini, C.; Brunelli, K. Effect of SiC and borosilicate glass particles on the corrosion and tribological behavior of AZ91D magnesium alloy after PEO process. *Surf. Coat. Technol.* **2021**, *428*, 127901. [[CrossRef](#)]
11. Li, C.; Zhu, D.; Cheng, S.; Zuo, Y.; Wang, Y.; Ma, C.; Dong, H. Recent research progress of bimetallic phosphides-based nanomaterials as cocatalyst for photocatalytic hydrogen evolution. *Chin. Chem. Lett.* **2022**, *33*, 1141–1153. [[CrossRef](#)]
12. Zhang, K.; Zhou, M.; Yang, K.; Yu, C.; Mu, P.; Yu, Z.; Lu, K.; Huang, W.; Dai, W. Photocatalytic H₂O₂ production and removal of Cr (VI) via a novel Lu₃NbO₇: Yb, Ho/CQDs/AgInS₂/In₂S₃ heterostructure with broad spectral response. *J. Hazard. Mater.* **2022**, *423*, 127172. [[CrossRef](#)]
13. Xu, M.Z.; Li, Q.; Lv, Y.Y.; Yuan, Z.M.; Guo, Y.X.; Jiang, H.J.; Gao, J.W.; Di, J.; Song, P.; Kang, L.X.; et al. Surfactant-assisted hydrothermal synthesis of MoS₂ micro-pompon structure with enhanced photocatalytic performance under visible light. *Tungsten* **2020**, *2*, 203–213. [[CrossRef](#)]
14. Sivaraman, C.; Vijayalakshmi, S.; Leonard, E.; Sagadevan, S.; Jambulingam, R. Current Developments in the Effective Removal of Environmental Pollutants through Photocatalytic Degradation Using Nanomaterials. *Catalysts* **2022**, *12*, 544. [[CrossRef](#)]
15. Motlagh, P.Y.; Khataee, A.; Hassani, A.; Rad, T.S. ZnFe-LDH/GO nanocomposite coated on the glass support as a highly efficient catalyst for visible light photodegradation of an emerging pollutant. *J. Mol. Liq.* **2020**, *302*, 112532. [[CrossRef](#)]
16. Morales-García, Á.; Valero, R.; Illas, F. Morphology of TiO₂ Nanoparticles as a Fingerprint for the Transient Absorption Spectra: Implications for Photocatalysis. *J. Phys. Chem. C* **2020**, *124*, 11819–11824. [[CrossRef](#)]

17. Carvalho, H.W.P.; Rocha, M.V.J.; Hammer, P.; Ramalho, T.C. TiO₂-Cu photocatalysts: A study on the long- and short-range chemical environment of the dopant. *J. Mater. Sci.* **2013**, *48*, 3904–3912. [[CrossRef](#)]
18. Moura, K.F.; Maul, J.; Albuquerque, A.R.; Casali, G.P.; Longo, E.; Keyson, D.; Souza, A.G.; Sambrano, J.R.; Santos, I.M.G. TiO₂ synthesized by microwave assisted solvothermal method: Experimental and theoretical evaluation. *J. Solid State Chem.* **2014**, *210*, 171–177. [[CrossRef](#)]
19. Silva Junior, E.; La Porta, F.A.; Liu, M.S.; Andrés, J.; Varela, J.A.; Longo, E. A relationship between structural and electronic order-disorder effects and optical properties in crystalline TiO₂ nanomaterials. *Dalt. Trans.* **2015**, *44*, 3159–3175. [[CrossRef](#)]
20. Substrates, Z.Z.; Boshkova, N.; Stambolova, I.; Stoyanova, D.; Simeonova, S.; Grozev, N.; Avdeev, G.; Shipochka, M.; Dimitrov, O.; Bachvarov, V.; et al. Protective Characteristics of TiO₂ Sol-Gel Layer Deposited on Zn-Ni or Zn-Co Substrates. *Coatings* **2023**, *13*, 295.
21. Wojcieszak, D.; Kapu, P. Influence of Annealing on Gas-Sensing Properties of TiO_x Coatings Prepared by Gas Impulse Magnetron Sputtering with Various O₂ Content. *Appl. Sci.* **2023**, *13*, 1724. [[CrossRef](#)]
22. Koppány, F.; Csomó, K.B.; Varmuzsa, E.M.; Bognár, E.; Pelyhe, L.; Nagy, P.; Kientzl, I.; Szabó, D.; Weszl, M.; Dobos, G.; et al. Enhancement of Hydrophilicity of Nano-Pitted TiO₂ Surface Using Phosphoric Acid Etching. *Nanomaterials* **2023**, *13*, 511. [[CrossRef](#)]
23. Stojadinović, S.; Radić, N.; Grbić, B.; Maletić, S.; Stefanov, P.; Pačevski, A.; Vasilić, R. Structural, photoluminescent and photocatalytic properties of TiO₂: Eu³⁺ coatings formed by plasma electrolytic oxidation. *Appl. Surf. Sci.* **2016**, *370*, 218–228. [[CrossRef](#)]
24. Lin, G.W.; Chen, J.S.; Tseng, W.; Lu, F.H. Formation of anatase TiO₂ coatings by plasma electrolytic oxidation for photocatalytic applications. *Surf. Coat. Technol.* **2019**, *357*, 28–35. [[CrossRef](#)]
25. Lu, X.; Schieda, M.; Blawert, C.; Kainer, K.U.; Zheludkevich, M.L. Formation of photocatalytic plasma electrolytic oxidation coatings on magnesium alloy by incorporation of TiO₂ particles. *Surf. Coat. Technol.* **2016**, *307*, 287–291. [[CrossRef](#)]
26. Tadić, N.; Stojadinović, S.; Radić, N.; Grbić, B.; Vasilić, R. Characterization and photocatalytic properties of tungsten doped TiO₂ coatings on aluminum obtained by plasma electrolytic oxidation. *Surf. Coat. Technol.* **2016**, *305*, 192–199. [[CrossRef](#)]
27. Lin, C.-C.; Krommenhoek, P.J.; Watson, S.S.; Gu, X. Chemical depth profiling of photovoltaic backsheets after accelerated laboratory weathering. *Reliab. Photovolt. Cells Modul. Compon. Syst. VII* **2014**, 9179, 91790R.
28. Geretschlager, K.J.; Wallner, G.M.; Fischer, J. Structure and basic properties of photovoltaic module backsheets. *Sol. Energy Mater. Sol. Cells* **2016**, *144*, 451–456. [[CrossRef](#)]
29. Cerchier, P.; Brunelli, K.; Pezzato, L.; Audoin, C.; Rakotoniaina, J.P.; Sessa, T.; Tammara, M.; Sabia, G.; Attanasio, A.; Forte, C.; et al. Innovative recycling of end of life silicon pv panels: Resielp. *Detritus* **2021**, *16*, 41–47. [[CrossRef](#)]
30. Trandafilović, L.V.; Jovanović, D.J.; Zhang, X.; Ptasinska, S.; Dramićanin, M.D. Enhanced photocatalytic degradation of methylene blue and methyl orange by ZnO: Eu nanoparticles. *Appl. Catal. B Environ.* **2017**, *203*, 740–752. [[CrossRef](#)]
31. Zuo, R.; Du, G.; Zhang, W.; Liu, L.; Liu, Y.; Mei, L.; Li, Z. Photocatalytic degradation of methylene blue using TiO₂ impregnated diatomite. *Adv. Mater. Sci. Eng.* **2014**, *2014*, 170148. [[CrossRef](#)]
32. Azeez, F.; Al-Hetlani, E.; Arafa, M.; Abdelmonem, Y.; Nazeer, A.A.; Amin, M.O.; Madkour, M. The effect of surface charge on photocatalytic degradation of methylene blue dye using chargeable titania nanoparticles. *Sci. Rep.* **2018**, *8*, 7104. [[CrossRef](#)]
33. Li, Q.B.; Liu, C.C.; Yang, W.B.; Liang, J. Growth mechanism and adhesion of PEO coatings on 2024Al alloy. *Surf. Eng.* **2017**, *33*, 760–766. [[CrossRef](#)]
34. Cerchier, P.; Pezzato, L.; Moschin, E.; Coelho, L.B.; Olivier, M.G.M.; Moro, I.; Magrini, M. Antifouling properties of different Plasma Electrolytic Oxidation coatings on 7075 aluminium alloy. *Int. Biodeterior. Biodegrad.* **2018**, *133*, 70–78. [[CrossRef](#)]
35. Shi, H.; Magaye, R.; Castranova, V.; Zhao, J. Titanium dioxide nanoparticles: A review of current toxicological data. *Part Fibre Toxicol* **2013**, *10*, 15. [[CrossRef](#)]
36. Lee, K.M.; Lee, B.U.; Yoon, S., II; Lee, E.S.; Yoo, B.; Shin, D.H. Evaluation of plasma temperature during plasma oxidation processing of AZ91 Mg alloy through analysis of the melting behavior of incorporated particles. *Electrochim. Acta* **2012**, *67*, 6–11. [[CrossRef](#)]
37. Gouma, P.I.; Mills, M.J. Anatase-to-Rutile Transformation in Titania Powders. *J. Am. Ceram. Soc.* **2001**, *84*, 619–622. [[CrossRef](#)]
38. Fattah-alhosseini, A.; Chaharmahali, R.; Babaei, K. Effect of particles addition to solution of plasma electrolytic oxidation (PEO) on the properties of PEO coatings formed on magnesium and its alloys: A review. *J. Magnes. Alloy.* **2020**, *8*, 799–818. [[CrossRef](#)]
39. Mashtalyar, D.V.; Imshinetskiy, I.M.; Nadaraia, K.V.; Gnedenkov, A.S.; Suchkov, S.N.; Opra, D.P.; Pustovalov, E.V.; Yu Ustinov, A.; Sinebryukhov, S.L.; Gnedenkov, S.V. Effect of TiO₂ nanoparticles on the photocatalytic properties of PEO coatings on Mg alloy. *J. Magnes. Alloy.* **2022**. [[CrossRef](#)]
40. Stojadinovic, S.; Radić, N.; Vasilić, R. Photoluminescent and Photocatalytic Properties of Eu³⁺-Doped MgAl Oxide Coatings Formed by Plasma Electrolytic Oxidation of AZ31 Magnesium Alloy Stevan. *Coatings* **2022**, *12*, 1830. [[CrossRef](#)]

Disclaimer/Publisher's Note: The statements, opinions and data contained in all publications are solely those of the individual author(s) and contributor(s) and not of MDPI and/or the editor(s). MDPI and/or the editor(s) disclaim responsibility for any injury to people or property resulting from any ideas, methods, instructions or products referred to in the content.